Coulomb Dissociation of Borromean Nuclei ^{17}B

Hyeji Lee

December 4, 2023

Abstract

Neutron-rich isotopes have received much attraction in recent years due to its structural properties such as neutron halo: one or two neutrons in the nucleus are weakly bound so that they are spatially extended far from the core nucleus. Borromean nuclei are particularly interesting due to the two-neutron halo structure. The Borromean nucleus is a bound three-body system, where any of its two-body subsystems are unbound. Experimental data of 2n halo structure has been reported for 6He, 11Li, and 19B. These 2n halo nuclei are possible to have a dineutron correlation, a spatially compact neutron pair, and the recent Coulomb dissociation of 19B revealed the dineutron in 19B. [1] We focus on 17B, which is also considered as a 2n halo nucleus. 17B is the core of the 2n halo nucleus 19B but 17B itself is the 2n halo nucleus. Investigating a dineutron correlation in the 17B will gives us a critical information about multi-neutron halo structure in neutron-rich isotopes. To investigate the dineutron correlation at the 17B, the experimental measurement using Coulomb dissociation was performed at SAMURAI (Superconducting Analyser for MUlti particles from RAdio Isotope beams) spectrometer in RIBF (Radioactive Isotope Beam Factory), RIKEN. A 48Ca primary beam accelerated to 345 MeV per nucleon was incident on a primary Be target to produce a 17B secondary beam. The generated secondary beam was separated and identified by BigRIPS fragment separator and was incident into a secondary Pb target where 17B is dissociated into 15B and two neutrons. The charged fragment 15B was detected by the SAMURAI spectrometer, while the two neutrons were detected by the neutron detectors NEBULA to measure Coulomb dissociation exclusive cross section. In this poster, we report the current analysis statue.

Contents

List of Figures

List of Tables

Chapter 1

Introduction

최근 몇년간, 가속기를 이용한 핵물리 실험이 급진적으로 발전함에 따라, 불안정 핵에 대한 연구가 급격하게 진행되었다. 특히 자연에서는 존재하지 않는 beta stability에서 먼, 원자핵의 존재 한계에 가까운 드립라인 핵에 대한 연구가 가능하게 되었다. 특히 양성자의 수보다 중성자의 수가 훨씬 많은 중성자 과잉 핵자에서는 안정 핵자에서는 볼 수 없는 특이한 현상들을 관찰 할 수 있는데, 중성자 헤일로가 대표적이다.

중성자 헤일로는 하나 또는 두개의 중성자가 코어로부터 공간적으로 멀리 떨어져있는 핵자다. 헤일로 중성자는 코어로부터 매우 약하게 속박되어 있고, 낮은 centrifugal barrier 를 갖고있는 낮은 궤도 각운동량 l=0 or 1를 갖고 있는 것이 특징이다. 이러한 특징으로 기인하는 중성자 헤일로 핵의 고유한 특징은 1MeV 이하의 아주 작은 중성자 분리 에너지 (안정핵은 보통 8MeV이다)와 주변핵자에 비해 매우 큰 반경, 그리고 Soft E1 Excitation이 있다. 그림1.1를 보면 원자번호 1부터 12까지의 핵자표가 있고, 원으로 표시된 핵자가 헤일로 핵자이다. 하나의 원은 1 중성자 헤일로, 2개의 원은 2중성자 헤일로이다. 지금까지 발견된 2중성자 헤일로는 6He, 11Li, 14Be, 17B, 19B, 22C로

Over recent years, The study of neutron-rich nuclei has garnered increasing attention within the field of nuclear physics, providing invaluable insights into the fundamental forces and interactions that govern atomic nuclei. Characterized by an excess of neutrons compared to stable isotopes, these nuclei serve as a compelling laboratory for investigating phenomena that transcend conventional nuclear models. One particularly intriguing subclass is that of 2-neutron halo nuclei, which feature an extended halo of two loosely bound neutrons.This thesis aims to delve deeper into the enigmatic properties and behaviors of 2-neutron halo nuclei, contributing to our broader comprehension of neutron-rich systems.

2 중성자 헤일로로 알 수 있는 것은 dineutron에 대한 연구이다. 본 논문에서는 납 타겟을 이용하여 17B를 Coulomb dissociation 시키고, 15B와 두 중성자를 검출하여 17B의 soft E1 Excitation을 조사하였다.

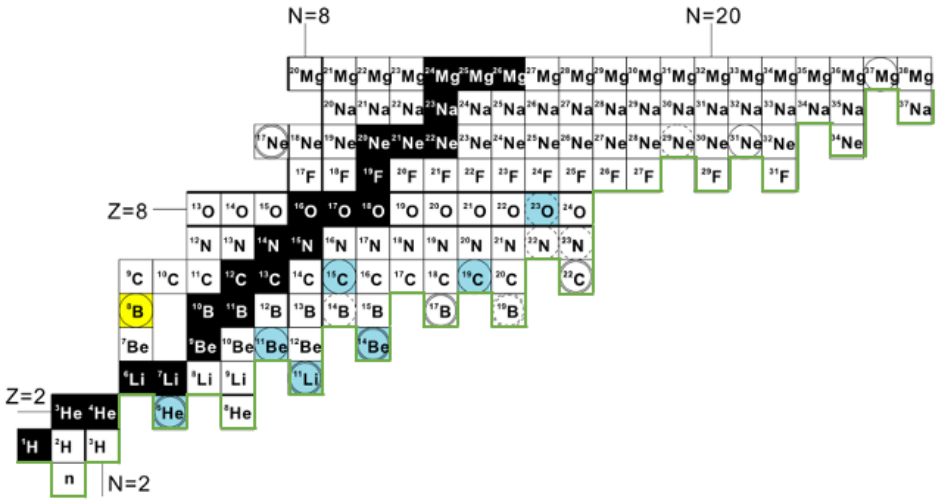

Figure 1.1: Nuclear Chart

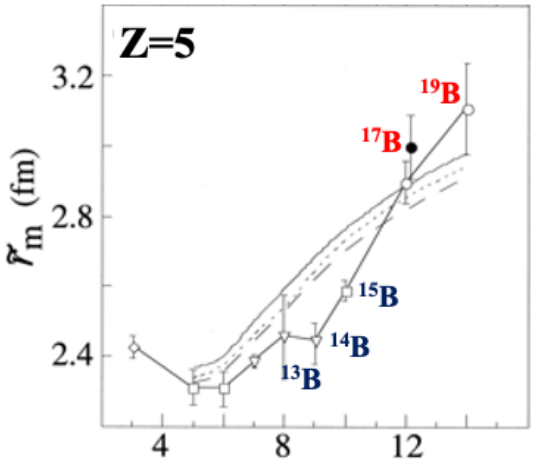

Chapter 2

Experimental Methods

이 장에서는 중성자 헤일로 핵의 구조상 특징에서 기인하는 soft E1 Excitation과 그것을 조사하는 방법인 Coulomb Dissociation에 대해 설명한다. 최종적으로, reduced transition probability B(E1)을 구하는 방법에 대해 설명한다.

2.1 Soft E1 Excitation in Neutron Halo Nuclei

왜 E1인지 설명

2.2 Coulomb Dissociation

2.2.1 Invariant Mass Method

납 타겟과 반응 직후 soft e1 excitation이 일어난 17b상태를 조사하기 위해서는 Invariant Mass Method로 상태를 재구성 할 필요가 있다. Excitation Energy는 다음과 같이 표시된다

$$E_x = S_{2n} + E_{rel}$$

여기서 S_{2n}은 중성자 분리 에너지, E_{rel}은 15B와 두 중성자 사이의 상대에너지이다.

2.2.2 Scattering Angle

2.3 Equivalent Photon Method

우리는 납과의 전자기적 반응이 일어날 때의 교환되는 가상 광자를 직접 검출 할 수 없다. 따라서 입사빔의 에너지와 타겟과의 거리, 타겟의 종류

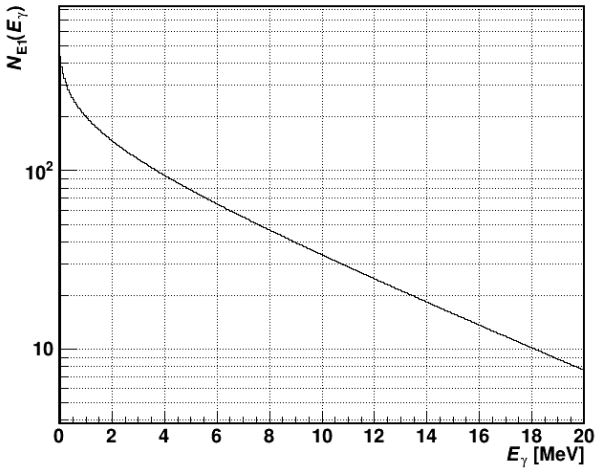
$N_{E1}(E_\gamma)$
10^2
10
0
2
4
6
8
10
12
14
16
18
20
E_γ [MeV]

Chapter 3

Experimental Setup

In this chapter, I will describe about beam, target, and detectors.

3.1 Production of ^{17}B beam

3.2 Experimental Setup overview

The experiment is

3.3 BigRIPS

3.3.1 Secondary Target

본 실험의 19B런에서는 카본 타겟과 납 타겟을 사용하였다. 카본 타겟의 두께는 10mm, 납 타겟의 두께는 1mm의 것과 2mm의 것을 겹쳐서 사용하였다.

3.3.2 BPC (Beam Proportional Chamber)

Magnetic Rigidity

3.3.3 Plastic Scintillator

TOF

3.3.4 Beam Drift Chamber

3.4 SAMURAI

3.5 Data acquisition system and Trigger condition

3.6 Run summary

hline Run number	Target	Trigger
394 - 404	C (1.8 g/cm^2)	DSB(1/20) + B x N + D(1/1)
405 - 409	Empty	DSB(1/20) + B x N + D(1/1)
410 - 427	Pb (3.0 g/cm^2)	DSB(1/20) + B x N + D(1/1)
428 - 431	Pb (3.0 g/cm^2)	DSB(1/20) + B x N + D(1/1)

3.7 Flight Length

Chapter 4

Data Analysis

In the analysis of experimental data, the primary goals are to extract the $2n$ removal cross section in the $^{17}\mathrm{B} \rightarrow {}^{15}\mathrm{B} + 2n$ reaction and to obtain the Relative energy spectrum. To achieve this, I will describe the procedure of identifying the secondary beam of ^{17}B, and selecting events involving the fragment ^{15}B and two neutrons. Particular emphasis is placed on the process of selecting two-neutron events and the rejection of cross-talk. The flow of the Data Analysis is as follows.

1. Select the event containing ^{17}B beam by beam PID
2. Select the event containing ^{15}B fragment by fragment PID
3. Select the event containing two neutron by cross-talk analysis
4. Extract the 2n removal cross section of the $^{17}\mathrm{B} \rightarrow {}^{15}\mathrm{B} + 2n$ reaction
5. Reconstruct Invariant Mass at target and obtain the Relative energy spectrum

4.1 Analysis of the Secondary Beam

The primary beam was generated by the SRC, RIBF. By accelerating ^{48}Ca to 345 MeV/u and bombarding it on a thick Be target (30mm), a secondary beam was produced. The characteristics of the primary beam were as follows. The collision between the initial beam and the target created the

Primary Beam	Beam Energy	Beam Intensity	Primary Target
^{48}Ca	345 MeV/u	210 pnA	Be (30mm)

Table 4.1: Information of Primary Beam

secondary beam, including not only the experiment's purpose isotope, ^{19}B, but also other neighboring isotopes. The main isotope used in this research is ^{17}B, which needed to be separated and identified through the BigRIPS separator. The identification of the ^{17}B secondary beam was performed using the TOF-Bρ-ΔE method. The identified ^{17}B was then transferred to SAMURAI, where it underwent Coulomb Dissociation, the main objective of this research. Three different targets were used: C, Pb, and Empty. The details for ^{17}B with each target were as follows.

4.1.1 Analysis of Time of Flight

The time-of-flight (TOF) is calculated using the time difference between two plastic scintillators. Three plastic scintillators are used for this TOF calculation. One is located at F7 and the other two, called SBT1 and SBT2, are at F13. The TOF between F7 and F13 is defined as following.

$$\mathrm{TOF}_{\mathrm{F7\text{-}F13}} = \frac{t_{\mathrm{SBT1}} + t_{\mathrm{SBT2}}}{2} - t_{\mathrm{F7}} + \Delta t_{offset} \tag{4.1}$$

isotope	Target	Average Energy at Target
^{17}B	C (1.789 g/cm2)	270 MeV/u
	Empty	275 MeV/u
	Pb (3.255 g/cm2)	270 MeV/u

Table 4.2: Information of Secondary Beam

Δt_{offset} is the offset used to correct for the difference between the actual measured $\text{TOF}_{\text{F7-F13}}$ and the TOF value calculated by considering the material between F7 and F13. For the calculation, runs with the f5 slit narrowed to ± 1mm (run number 428,429,431) are used,for the mono-energetic isotopes. The calculated $\text{TOF}_{\text{F7-F13}}$ value is 192.333 ns, and the corresponding Δt_{offset} value is 172.025 ns. tof 분해능 추가

4.1.2 Analysis of Magnetic Rigidity

Magnetic Rigidity $B\rho$ is derived by Beam Projection Chamber (BPC) located at dispersive focal plane (F5). The x position of a beam passing through F5 is measured by BPC, and the $B\rho$ is calculated using the following equation.

$$B\rho = (1 + \frac{x}{D})B\rho_0 \tag{4.2}$$

with the rigidity of the central trajectory $B\rho_0$, 8.78 Tm, and momentum dispersion D, 3300 cm/%. The position resolution of BPC is ooo from wire spacing 4 mm. Brho의 분해능 추가

4.1.3 Analysis of Energy Loss

The energy loss ΔE is measured in the Ionize Chamber for Beam (ICB). The correlation between ΔE and Z can be obtained according to the simplified Bethe-Bloch's Energy loss formula as follows. In this formula, the*density effect* correction δ or *shell* correction C is skipped.

$$\frac{dE}{dx} = 2\pi N_a r_e^2 m_e c^2 \rho_{\text{P10}} \left(\frac{Z_{\text{P10}}}{A_{\text{P10}}}\right)\left(\frac{Z^2}{\beta^2}\right)\left[\ln\frac{2m_e c^2\beta^2\gamma^2}{I_{\text{P10}}} - \beta^2\right] \tag{4.3}$$

with

$$2\pi N_a r_e^2 m_e c^2 \rho_{\text{P10}} = 0.307075 \text{ MeV cm}^2\text{g}^{-1} \tag{4.4}$$

N_a : Avogadro's number = 6.022×10^{23}
r_e : classical electron radius = 2.817×10^{-13} cm
m_e : electron mass = 0.511 MeV/c^2
ρ_{P10} : density of the P10 gas = 1.84×10^{-3} g/cm^3
Z_{P10} : effective atomic number of the P10 gas
A_{P10} : effective mass number of the P10 gas
I_{P10} : mean excitation energy of the P10 gas
$\beta = v/c$ of the beam particle
$\gamma = 1/\sqrt{1-\beta^2}$

Because of the P10 gas is compound of 90% Ar and 10% CH_4, the mean excitation energy I_{P10} is calculated as follows. The detail of the calculation of I for compound is described in the Appendix A.

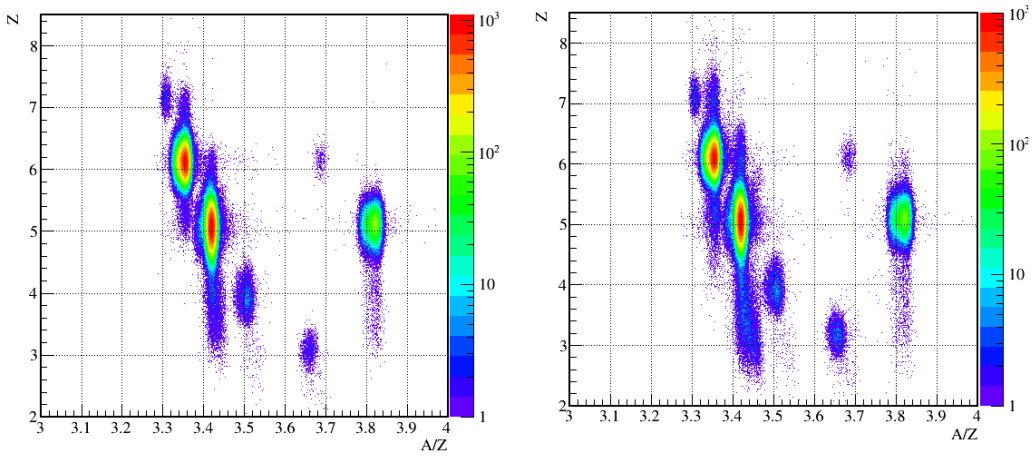

Figure 4.1: Beam Particle Identification for Pb target (left) and C target (right)

4.1.4 Beam Particle Identification

Secondary beam particles are identified using the TOF-Bρ-ΔE method. A/Z and Z is driven by the following equation.

$$\beta_{\mathrm{TOF}} = L(\text{F7-F13})/(\mathrm{TOF}_{\text{F7-F13}} \times c) \tag{4.5}$$

$$\beta_{\mathrm{F5}} = f(\mathrm{TOF}_{\text{F7-F13}}) \tag{4.6}$$

$$A/Z = cB\rho_{\mathrm{F5}}\gamma_{\mathrm{F5}}/m_u\beta_{\mathrm{F5}} \tag{4.7}$$

β_{F5} is polynomial function of

$$Z = \beta_{\mathrm{TOF}}\sqrt{\Delta E_{\mathrm{ICB}}/(0.307075 \times \Delta x \times (Z_{\mathrm{P10}}/A_{\mathrm{P10}})\ln(2m_e c^2\beta^2\gamma^2/I_{\mathrm{P10}} - \beta^2))} \tag{4.8}$$

ΔE_{ICB} is total energy loss at ICB and Δx is the thickness of ICB. Figure 4.1 shows the histogram of particle identification of the secondary beam with x-axis as A/Z and y-axis as Z.

Secondary Beam	Pb target	C target	Empty target
^{19}B	2	3	4
^{17}B			
^{20}C			

Table 4.3: statistic of Secondary Beam

Following table shows each particle's statistic and Intensity

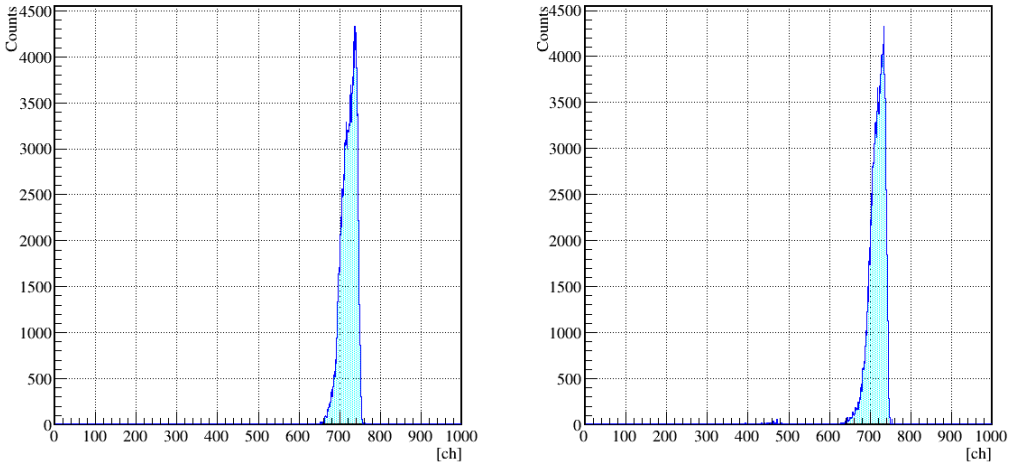

Figure 4.2: TDC Distribution of BDC1 (left) and BDC2 (right)

4.2 Beam Profile at Target

The beam profile at the target can be determined using two drift chambers, BDC1 and BDC2, located upstream of the target. BDC1 and BDC2 are Ionized Drift Chambers that allow for the determination of a particle's trajectory through reconstruction of the hit positions on each layer. By using this feature, the incident position and angle at the each BDC can be determined, and these are then extrapolated to find the incident position and angle at the target.

4.2.1 BDC Calibration

TDC Distribution

The timing information of the BDC is obtained using the TDC. And using this information, we can calculate the drift distance This TDC distribution is obtained from run 431 which is f5 slit is

	t_{min} [ch]	t_{max} [ch]
BDC1	600	800
BDC2	600	800

Table 4.4: TDC window of BDC1 and BDC2

Drift Chamber의 각 레이어에 검출된 위치 (x,y)를 통해 입자의 통과 궤적을 선형 fitting 으로 구할 수 있다. 이 궤적을 통해 각각의 layer에서의 위치가 Reconstruct된다. STC (Space-Time Conversion) function 를 이용하여 각 layer에서의 위치와 시간을 통해 입자의 통과 궤적을 구할 수 있다.

$$\frac{dN}{dx} = const. \tag{4.9}$$

Then STC function is derived as follows.

$$\frac{dN}{dt} \cdot \frac{dt}{dx} = const. \tag{4.10}$$

$$dx = C \cdot \frac{dN}{dt} \cdot dt, \tag{4.11}$$

$$x(t) = C \cdot \int_{t_0}^{t} \frac{dN}{dt} dt \tag{4.12}$$

$$\delta x = x_{calc} - x_{hit} \tag{4.13}$$

4.2.2 Beam Profile at Target

Target Chamber 주변에는 검출기가 없기 때문에 두개의 BDC를 이용하여 target에서의 Beam 위치를 외삽한다. 본 실험에서 사용하는 ^{17}B는 본 실험의 main beam이 아니기 때문에, 위에서 확인한 BDC에서의 beam profile 과 같이 target 중심에서 ずれている 따라서 Target의 유효면적 x +/- 35mm, y +/- 35mm를 정의하고, 이를 넘어가는 이벤트는 제거한다.

4.2.3 Beam beta calculation

Invariant Mass를 계산하기 위해서는 Beam의 beta를 계산해야 한다. Beam의 beta는 다음과 같이 계산된다.

Eloss Calculation

Once TOF_{F7-F13} has been calculated, the β_{beam} can be calculated using the following equation.

$$\beta_{F7-F13} = \frac{L(F7 - F13)}{TOF_{F7-F13} \times c} \tag{4.14}$$

차후의 Invariant Mass 계산을 위해 target 중심에서의 beam-beta를 구할 필요가 있다. F5에서의 Brho를 beta는 tof713의 이차식으로 다음과 같이 나타낼 수 있다. 또한 각 특정 위치에 대한 coefficient는 표에 표시하였다.

$$TOF_{F7_{Tgt}} = aTOF^2_{F7-F13} + bTOF_{F7-F13} + c\beta_{F5} \tag{4.15}$$

	t_{min} [ch]	t_{max} [ch]
FDC1	600	800
FDC2	600	800

Table 4.5: TDC window condition of FDC1 and FDC2

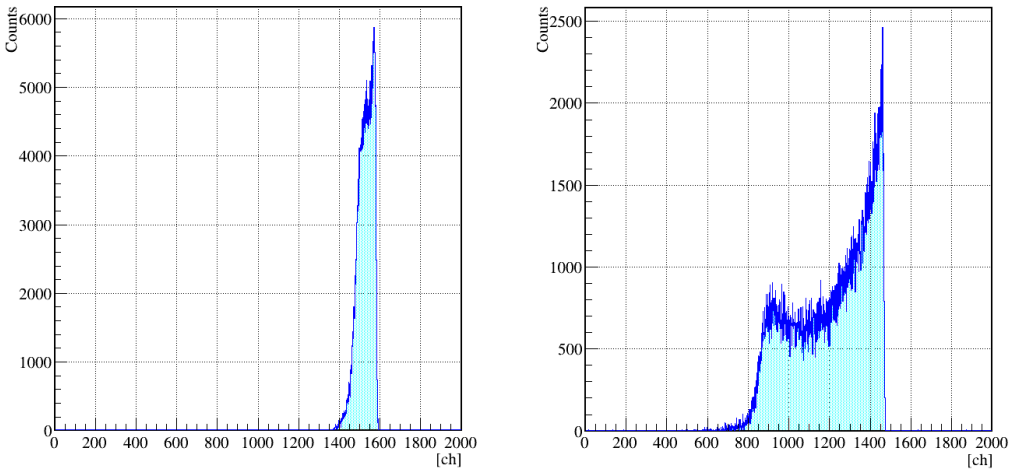

Figure 4.3: TDC Distribution of FDC1 (left) and FDC2 (right)

4.3 Analysis of charged fragment

4.3.1 FDC를 이용한 위치 계산

4.3.2 Brho from Simulation

Simulation Using Monte Carlo Method

Numerical Calculation

Optrace는 Magnetic Field 데이터를 기반으로 입자의 Transformation Matrix를 구하는 프로그램이다. 본 실험에서 사용된 SAMURAI의 profile은 3T의 중심자기장과 60도의 회전각도를 갖는다. 이를 기반으로 Optrace 자기장 파일을 작성한 결과, 자기장에 대한 Transformation Matrix는 다음과 같다.

4.3.3 HODscope Z

15B를 특정하기 위하여, Hodscope라는 Plastic Scintillator 검출기에서 Z를 특정한다. 상류에서 17B를 특정하여, 가장 많은 입자가 Z=5라고 가정, 위의 시뮬레이션으로 얻은 AOZ를 대입하여 15B를 특정한다.

4.3.4 Fragment Particle Identification

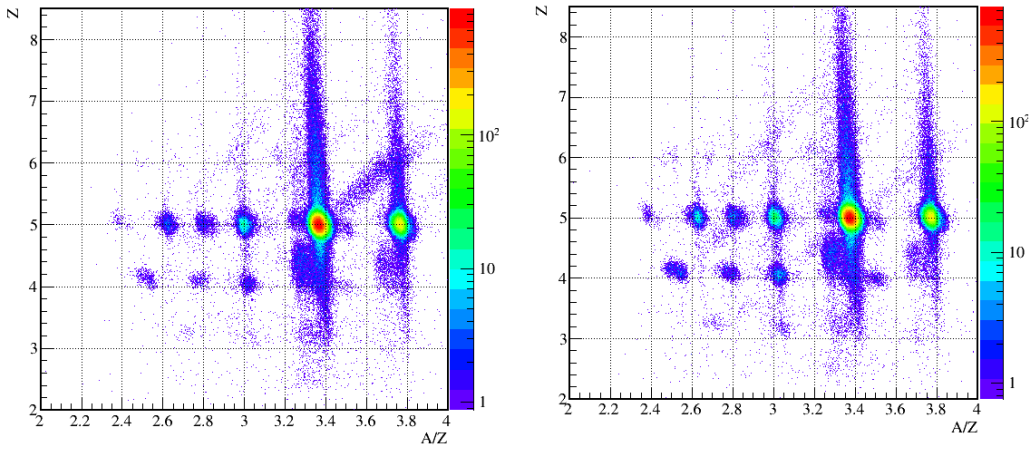

Figure 4.4: Fragment Particle Identification of All Events at Pb target (left) and C target (right)

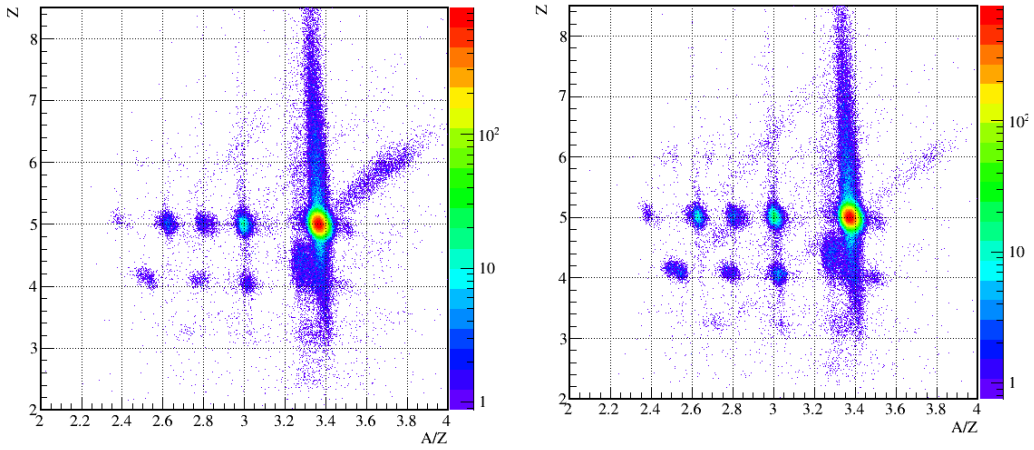

Figure 4.5: Fragment Particle Identification of ^{17}B Events at Pb target (left) and C target (right)

4.4 Analysis of Neutrons

A neutron is detected indirectly by recoiled charged particles which is mainly produced by H(n,n) and ^{12}C(n,np) reaction in the plastic-scintillator.

In this experiment, neutrons emitted from the secondary beam ^{17}B are detected by the NEBULA neutron detector system within the SAMURAI setup. This section describes the process of selecting either single-neutron or two-neutron events using the NEBULA neutron detector array. The momentum $P(n)$ of the neutron is reconstructed from the detection position in NEBULA relative to the target, and the time-of-flight (TOF). The energy of the neutron is described as follows.

$$L = |\vec{r}_{\rm tgt} - \vec{r}_n| \tag{4.16}$$
$$\beta_n = L/({\rm TOF}_{\rm NEB\text{-}tgt} \times c) \tag{4.17}$$
$$P_n = m_n \beta_n \gamma_n \tag{4.18}$$
$$E_n = m_n \gamma_n \tag{4.19}$$
$$\vec{P_n} = \frac{\vec{r_n} - \vec{r_n}}{L} P_n \tag{4.20}$$

where, $\vec{r}_{\rm tgt}$ is the position of the target $\vec{r}_{\rm tgt} = ()$, m_n is the neutron mass (m_n = MeV)

4.4.1 Selection of Neutron Events

Because of the indirect detection of neutrons, the selection of neutron events is more complicated than that of charged particles. The selection of neutron events is performed in four steps. First, reject the events which assumed as gamma event. Second, reject the events which is assumed as recoiled proton or gamma event. Third, in two neutron selection case, remove the event which is assumed as cross-talk. After all, select the fastest and second fastest event as a real neutron event.

gamma event rejection

진짜 뉴트론 이벤트를 선택하기 위해서 감마선을 제거하는 스레숄드를 지정한다.

1. 1st VETO에 hit한 이벤트는 모두 하전입자라 간주하여 제거한다.

2. 중성자 검출기 NEBULA에 입사한 이벤트 중, 발광량 Q가 6MeVee 이하인 이벤트는 감마선으로 간주하여 제거한다. 또한 하나의 플라스틱 신틸레이터 모듈을 통과할 때의 중성자의 최대 에너지 loss 130MeV를 넘어가는 이벤트도 중성자에서 산란된 다른 이벤트로 간주하여 제거한다.

3. Target에서부터의 TOF가 1st wall의 경우 40ns 이하, 2nd wall의 경우 42ns 이하인 이벤트 또한 중성자 이외의 이벤트로 간주하여 제거한다.

4. (2중성자 이벤트에 대해서만) 2nd VETO에 hit한 이벤트에 대하여, 2nd NEUT wall에 입사한 가장 빠른 두 중성자 이벤트가 dr(xy)¡500mm, 2ns ¡dt¡ 5ns 인 이벤트는 2nd VETO에서 기인한 cluster 산란 이벤트로 간주하여 제거한다.

When selecting events of two neutrons, the most important process is the elimination of cross-talk. Cross-talk refers to the phenomenon where a single neutron generates multiple signals, which Cross-talk is the most significant source of noise when selecting two-neutron events.
Cross-talk 제거에는 크게 3가지 단계가 있다. To reject cross-talk, a Geant4 simulation was performed to generate events of $^{16}{\rm B} \rightarrow {}^{15}{\rm B} + n$, thereby replicating cases where all two-neutron events are due to cross-talk. The details of the executed Geant4 simulation are as follows.

Reaction	$^{16}\mathrm{B} \rightarrow {}^{15}\mathrm{B} + n$
Beam Energy	140 MeV/u
Relative Energy	0 - 10 MeV (Uniformly Generated)
Position Distribution	Reconstructed from ^{17}B Beam profile
Angular Distribution	Reconstructed from ^{17}B Beam profile

4.4.2 Clustering Event Subtraction

4.4.3 same wall event

두 중성자

cluster proton cross-talk

4.4.4 different wall

4.5 Cross-talk 잔존률 평가

각각의 Cross talk 제거 단계에 따라 Cross-talk가 남아있는 비율을 평가하였다. 단계는 4단계로 나누어, 다음과 같이 구분한다.

1. (a) no rejection
2. (b) clustering rejection
3. (c) clustering rejection + same wall rejection
4. (d) clustering rejection + same wall rejection + gamma rejection

각 단계에서의 Cross-talk 잔존률은 다음과 같은 식으로 나타낸다.

$$R = \frac{N_{M>2}}{N_{M>1}} \tag{4.21}$$

1n 시뮬레이션에서 잔존률 1%를 목표로 분석을 진행하였다. 분석 결과 전체 M¿1 event 225385 이며, 각 단계에서의 M¿2 event와 잔존률 R은 다음과 같다. 조건 d까지 적용하였을 때 각각의 Wall에서 잔존률이 1% 이하로 낮아지는 것을 확인할 수 있다.

Condition	same wall event (R)	different wall event (R)	all wall event (R)
(a)	89721 (39.8%)	10123 (4.5%)	99844 (44.3%)
(b)	29032 (12.9%)	16848 (7.5%)	45880 (20.4%)
(c)	6274 (2.8)%)	2791 (1.2%)	9065 (4.0%)
(d)	5352 (2.4%)	2089 (0.9%)	7441 (3.3%)

4.6 Acceptance and Efficiency Correction

SAMURAI의 Acceptance and Efficiency를 평가하기 위해 Geant4 Simulation을 진행했다. 시뮬레이션 정보는 다음과 같다

Physics Model	Phase Space Decay
Beam Energy	270 MeV/u
Relative Energy	1-10 MeV (Uniformly generated)

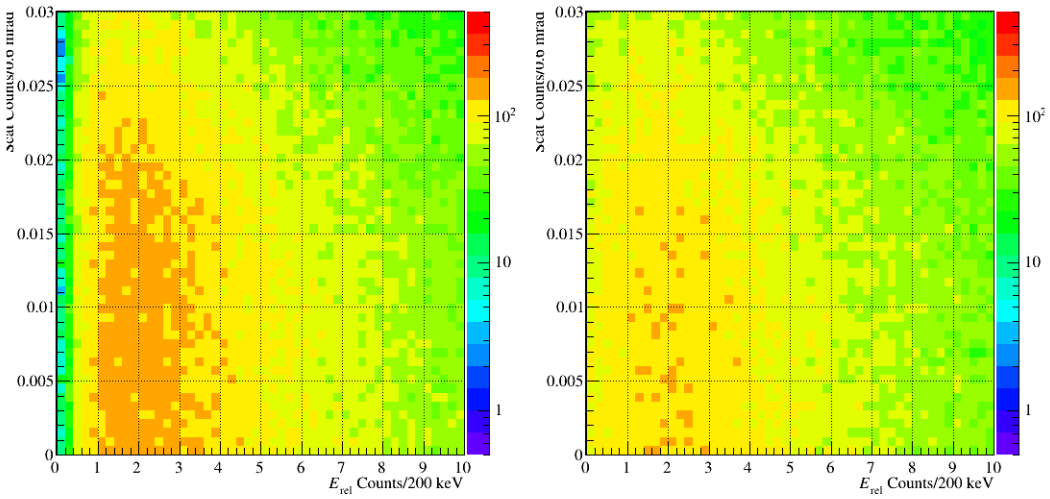

Figure 4.6: 2n Acceptance for same wall (left) and different wall (right)

4.7 Experimental Resolution

4.8 Relative Energy Spectrum

4.9 Exclusive Cross Section

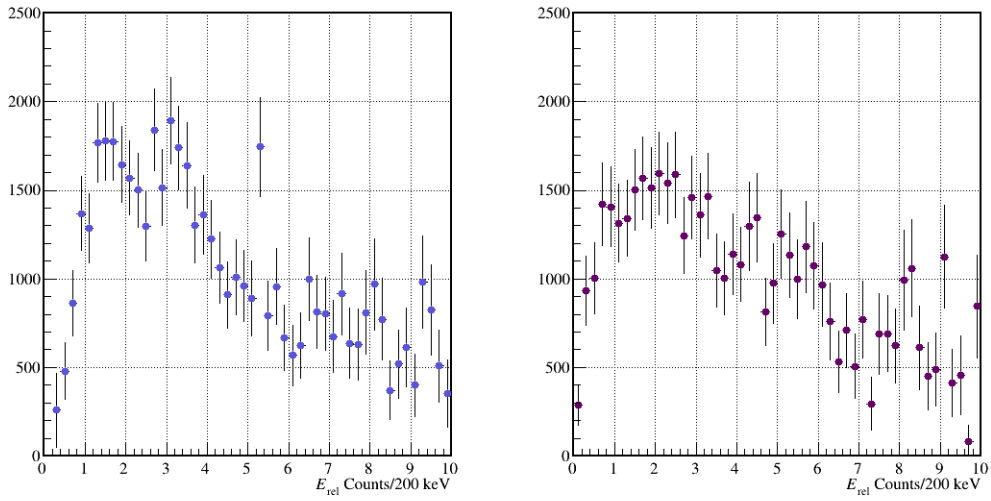

Figure 4.7: Relative Energy Spectrum of Pb target

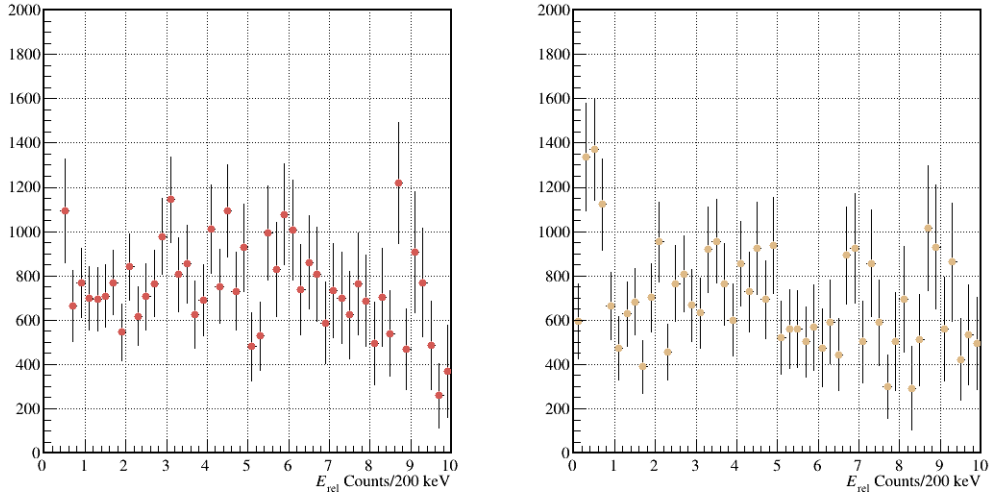

Figure 4.8: Relative Energy Spectrum of C target

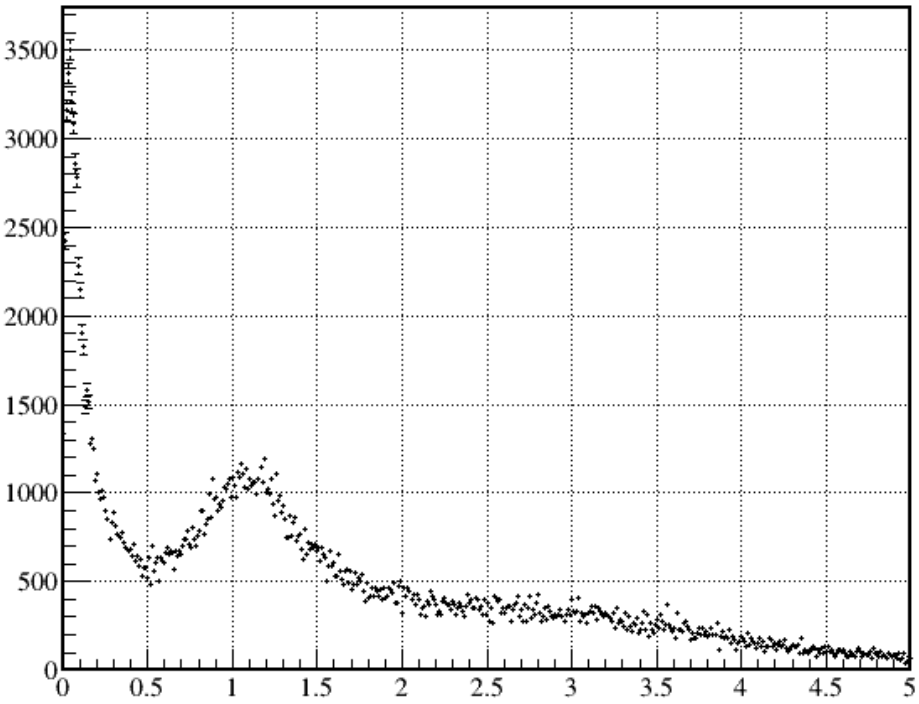

Figure 4.9: Relative Energy Spectrum of ^{16}B + n at C target

Chapter 5

Result and Discussion

In this chapter, we discuss about the results obtained through data analysis.

5.1 Inclusive Cross Section

5.2 Neutron Removal Cross Section

	σ_{incl} (mb)	σ_{-2n} (mb)	σ_{-4n} (mb)
^{17}B + Pb		713()	
^{17}B + C		149()	
σ_{Pb}/σ_C			

Table 5.1: Reaction Cross Section of Boron Isotopes

5.3 Relative Energy Spectrum

5.4 Coulomb Dissociation Cross Section

Coulomb dissociation cross section can be extracted by using the following equation.

$$\sigma_{CD} = \sigma_{incl}(Pb) - \Gamma\sigma_{incl}(C) \tag{5.1}$$

We used Γ value from calculation .

	Γ	σ_{coul}
^{17}B	2.385	281 $\pm$ 8 mb

Table 5.2: Coulomb Dissociation Cross Section

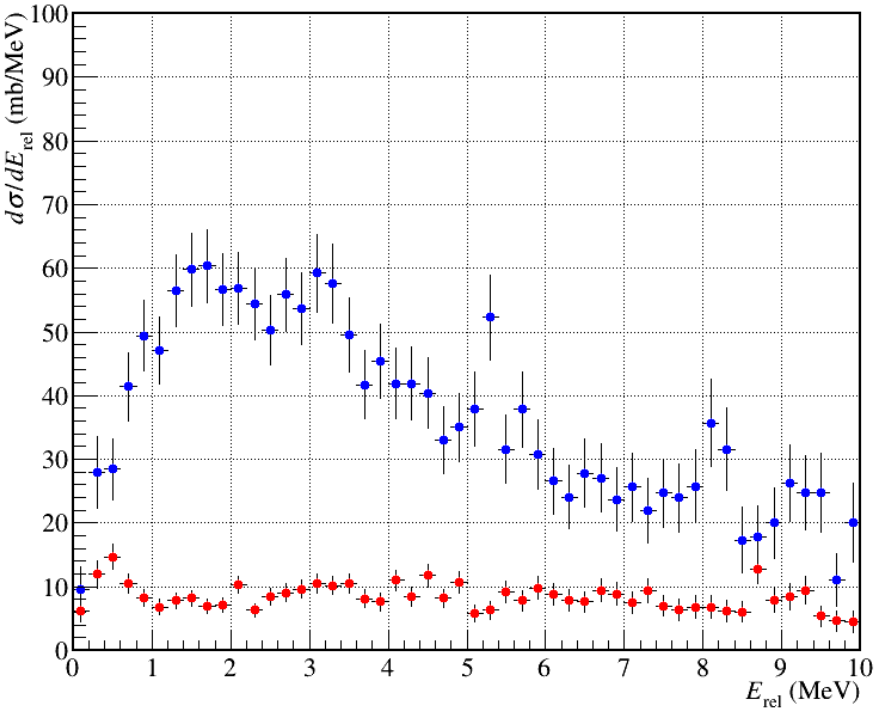

Figure 5.1: Cross Section

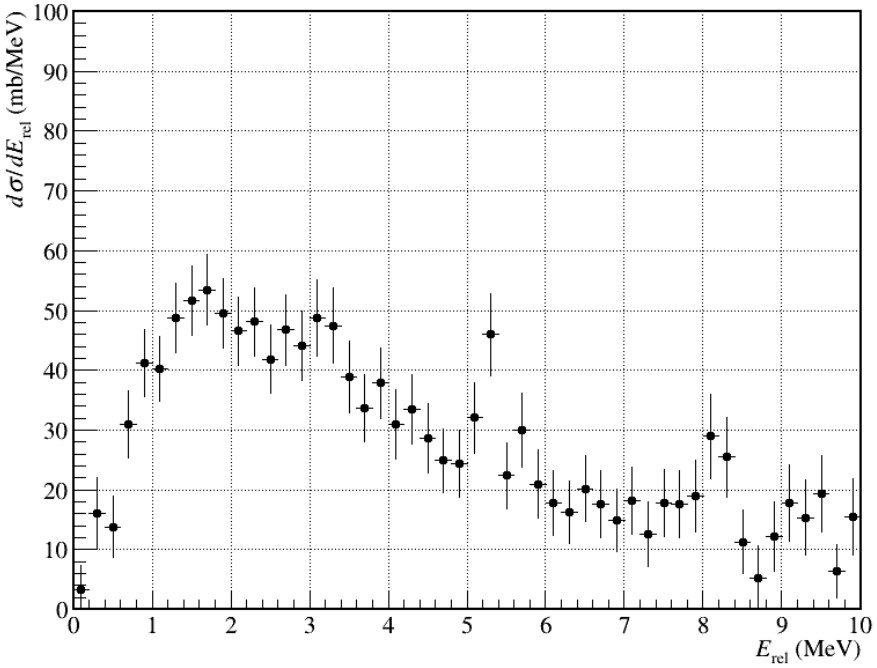

Figure 5.2: Coulomb Dissociation Cross Section

About reduced dipole transition probability, we can extract $B(E1)$ strength as follows.

$$\frac{d\sigma_{coul}}{dE_x} = \frac{16\pi^3}{9\hbar c} N_{\mathrm{E1}}(E_x) \frac{dB(\mathrm{E1})}{dE_x} \tag{5.2}$$

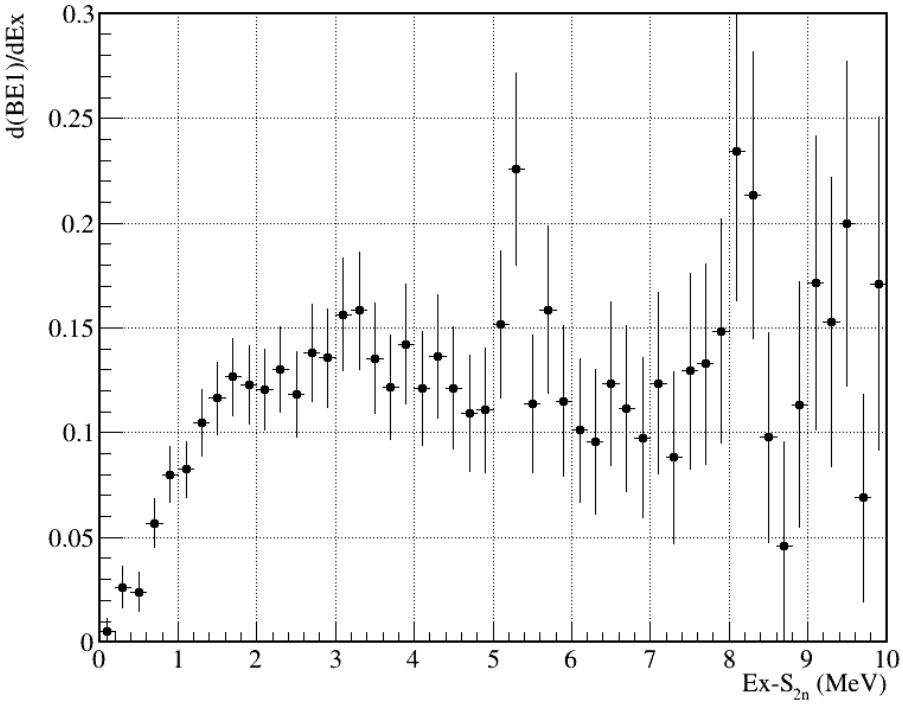

Figure 5.3: B(E1) Strength

$$B(E1) = \int_0^{+\inf} \frac{dB(E1)}{dE_x} dE_x \tag{5.3}$$

$$= \int_0^{+10} \frac{dB(E1)}{dE_x} dE_x \tag{5.4}$$

$$= 1.22 \pm 0.06 [e^2 fm^2] \tag{5.5}$$

5.5 Dineutron Correlation

$$B(E1) = \frac{3}{\pi} \left(\frac{Ze}{A} \right)^2 \langle r^2_{c-nn} \rangle \tag{5.6}$$

With the obtained $B(E1)$ strength up to 10 MeV, we can extract $\sqrt{\langle r^2_{c-nn} \rangle}$ as follows.

$$\sqrt{\langle r^2_{c-nn} \rangle} = 0.00 \pm 0.00(stat.) \pm 0.00(syst.) \text{ fm} \tag{5.7}$$

Furthermore, we can extract the distance of $2n$ from three body model.

$$\langle r^2_{halo}\rangle = \frac{A_c}{A}\langle r^2_{core}\rangle + \frac{2A_c}{A^2}\langle r^2_{c-nn}\rangle - \frac{1}{2A}\langle r^2_{nn}\rangle \tag{5.8}$$

where A and A_c is the mass number of halo nucleus and core. $\langle r^2_h\rangle$ and $\langle r^2_c\rangle$ are the mean-square matter radius of halo nuclei and the core, which is 3.00(6) fm and 2.75(6) fm respectively.

$$\sqrt{\langle r^2_{nn}\rangle} = 3.20 \pm 0.00(stat.) \pm 0.00(syst.)\ \text{fm} \tag{5.9}$$

Finally, the mean opening angle of dineutron can be extracted as follows.

$$\langle \theta_{nn}\rangle = 6.57 \pm 0.00(stat.) \pm 0.00(syst.)\ \text{deg.} \tag{5.10}$$

Chapter 6

Conclusion

Spectroscopy of 17B is ...

Appendix A

Equations

A.1 Bethe-Bloch Formula

Energy loss calculation for

A.2 Equivalent Photon Method

considering multi-polarity,

$$n_{\pi l}(\omega) = Z_1^2 \alpha \frac{l[(2l+1)]!!^2}{(2\pi)^3(l+1)} \sum_m \left| G_{\pi lm}\left(\frac{c}{v}\right) \right|^2 g_m(\xi)$$

equivalent photon number for E1 excited projectile.

$$n_{E1}(\omega) = n_{E1,m=-1} + n_{E1,m=0} + n_{E1,m=+1} = \frac{2}{\pi} Z_1^2 \alpha \Big(\frac{c}{v}\Big)^2 \Big[\xi K_0(\xi) K_1(\xi) - \frac{v^2 \xi^2}{2c^2}(K_1^2(\xi) - K_0^2(\xi)\Big]$$

with

$$\xi = E_\gamma R/\gamma\nu\hbar \tag{A.1}$$

$$E_\gamma : Photonenergy(E_\gamma = \omega\hbar) \tag{A.2}$$

$$Z_1 : Atomicnumberoftarget \tag{A.3}$$

R: impact parameter (1.3)

Appendix B

Appendix B

B.1 Resolution Evaluation

Flight length	Distance
F7-F13	7.5m
dist-BDC1-BDC2	1.5m
dist-BDC1-tgt	1.5m
target z	0.5m
dist-FDC1-Tgt	1.5m
dist-FDC2-HOD	1.5m

Table B.1: Flight length